

# Improving the Seismic Performance of an 8-storey RC Frame Using GFRP

**A. Eslami & H.R. Ronagh**

*University of Queensland, Australia*



## SUMMARY:

A numerical investigation was conducted on the efficiency of glass fibre reinforced polymers (GFRP) in improving the seismic performance of RC frames. For this purpose, an 8-storey frame is considered with different levels of transverse reinforcement representing well-confined and poorly-confined conditions. Despite GFRP wrapping of columns at the critical regions considered as the main retrofitting technique in this paper, effect of increasing the beam ductility in seismic performance of the structure is also evaluated for the code-compliant frame. The aim of retrofitting is to provide both columns and beams with more ductility. The pushover results are then implemented in the seismic analysis using the capacity spectrum method. The results show the efficiency of FRP wraps in improving the seismic performance and ductility of the poorly-confined frame, while for the code-compliant buildings, increasing the lateral load carrying capacity or beam ductility could be considered as more efficient techniques.

*Keywords: GFRP, seismic retrofitting, ductility, nonlinear plastic hinge, pushover analysis*

## 1. INTRODUCTION

It is evident that many existing buildings have yet to be retrofitted in order to remain reasonably intact and safe during pulse-type ground motions or more severe earthquakes than those they have been designed for. In addition to near-fault earthquakes, changes in seismic hazard levels, design methods, and serviceability requirements, are amongst other reasons for retrofitting a code-compliant or deficient structure subjected to an ordinary earthquake.

During the last couple of decades, application of composite materials for retrofitting/upgrading of reinforced concrete (RC) buildings has experienced a sharp increase. Compared to other building materials, FRPs offer several advantages; such as, possessing high tensile strength, low specific weight, high resistance to corrosion, and ease of application. In an experimental study, Balsamo *et al.* (2005) assessed the seismic performance of a full-scale RC structure repaired using carbon fibre reinforced (CFRP) laminates and wraps. Their results proved that a large displacement capacity exists in the repaired structure while no reduction of strength was seen after the application of FRP at beam-column joints and walls. In another experimental study, Di Ludovico *et al.* (2008) investigated seismic retrofitting of an under-designed, full-scale RC structure with FRP wrapping. Their research confirmed the effectiveness of FRP in confining effects to improving the global performance of a structure in terms of ductility and energy dissipating capacity. Recently, Niroomandi *et al.* (2010) investigated the seismic performance of an ordinary RC frame. Their pushover analysis showed that relocating plastic hinges away from the column faces through web-bonded FRP retrofitting of joints in an 8-storey frame increased the lateral load carrying capacity and seismic behaviour factor by 40% and 100%, respectively. However, it is worth mentioning that web-bonded technique comes with certain limitations in practical applications.

This paper aims to evaluate the efficiency of FRP composites applied at the critical regions of RC

members used to enhance the seismic performance of RC structures. The method is to increase the ductility of plastic hinges at beam and column ends without varying their strength levels. Technically speaking, in the latter case, flexural strengthening of columns and beams with proper anchorage of composite sheets are necessary. An 8-storey RC building is used as the case study structure. Torsion effects have been neglected in this study and two-dimensional (2-D) frames analyzed as being representative of regular RC buildings. The frame was detailed based on two different reinforcement spaces resulting in two RC frames with different levels of transverse steel reinforcement. Hereafter, these two structures are called “intermediate” and “poorly-confined” frames. The nonlinear static (pushover) analysis was performed in order to estimate the seismic response of the structures. In addition, the concept of lumped plasticity was used in the characterization of nonlinear properties of members. A finite element analysis program, SAP 2000 (Computers and Structures *Inc*, 2009), commonly used by structural engineering professionals, was utilized to run the nonlinear static analysis. The N2 method (Fajfar, 2000) was employed in order to evaluate the seismic demand and capacity of the retrofitted and original frames.

## 2. DESIGN AND DESCRIPTION OF THE FRAMES

The structure considered was an 8-storey moment resisting RC frame representing a mid-rise building. The frame considered to be part of the lateral resisting system of a residential building with three bays (each equal to 5 m). The height was assumed to be equal to 3 m for all stories. The seismic loads were considered according to the provisions of the Iranian seismic code (Iranian code of practice for seismic resistant design of buildings, 2005). In the design of the moment resisting frame, the design dead load and live load were assumed to be equal to 30 *kN/m* and 10 *kN/m*, respectively, which were applied to the beams in addition to the self-weight of the structure. In addition, the compressive strength of concrete was taken as 25 *MPa* and deformed bars of Grade 60 ( $f_y = 420$  *MPa*) were considered as steel reinforcement. Design base shear was determined considering a peak ground acceleration of 0.3g representing a high seismic hazard and soil type-III which is similar to class *D* of FEMA-356 (American Society of Civil Engineering, 2000).

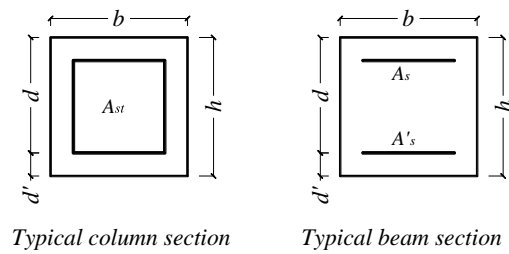
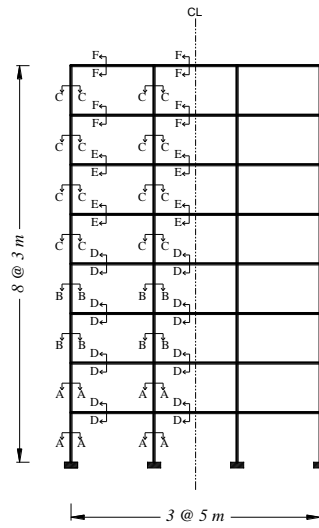


**Figure 2.1.** Distribution of longitudinal reinforcement in a typical beam and column section

In order to investigate the confinement effect of steel, the frame was reinforced at two different transverse reinforcement levels creating two distinct frames that are called “intermediate” and “poorly-confined” as mentioned previously. The former was detailed based on the intermediate provisions of the ACI 318-02 (ACI Committee 318, 2002), whereas in the latter only the shear design was considered for transverse reinforcing. The poorly-confined frame represents the situations in which the current code provisions are not satisfied. The longitudinal reinforcements in both frames were similar as they were designed for similar gravity and seismic load levels. For both frames, deformed steel bar, 10 mm in diameter, was selected as transverse reinforcement. The fundamental period of the structure was calculated to be around 1.28 s. As shown in Fig. 2.1, for a typical beam and column section, the column longitudinal reinforcement was distributed around the section, while the beam longitudinal bars were positioned at the top and bottom of the section in all frames. Fig. 2.2 provides a schematic illustration along with the dimensions and flexural/transverse reinforcement of the members in both considered frames.



Section	$b$	$h$	$d$	$d'$	$A_{st}$	$A_s$	$A'_s$	Transverse steel spacing (mm)	
								Intermediate frame	Poorly-confined frame
A-A	600	600	540	60	16 $\phi$ 25	-	-	150	450
B-B	600	600	540	60	16 $\phi$ 18	-	-	150	450
C-C	500	500	440	60	16 $\phi$ 16	-	-	125	450
D-D	500	500	440	60	-	6 $\phi$ 25	4 $\phi$ 25	100	140
E-E	500	500	440	60	-	6 $\phi$ 22	4 $\phi$ 22	100	175
F-F	500	500	440	60	-	6 $\phi$ 18	3 $\phi$ 18	100	250

**Figure. 2.2.** Reinforcement details of the 8-storey intermediate frame and poorly-confined frame

### 3. NONLINEAR ANALYSIS OF THE FRAMES

In this section, after verification of the adopted assumptions and nonlinear analysis results, the pushover analyses of the selected frames were carried out in SAP 2000 (Computers and Structures *Inc.*, 2009) and the base shear- roof displacement obtained for each frame as a characteristic force-displacement curve.

#### 3.1. Lumped Plasticity Modeling of the Frames

The moment-curvature properties of the plastic hinges were determined using XTRACT software (Imbseon and Associates *Inc.*, 2011). This program calculated the moment-curvature relationship based on fibre analysis of the end sections in the beams and columns considering section properties, reinforcement details and a constant axial load. Axial loads on the columns were assumed to be equal to the resultant loads calculated from dead loads plus 20% of live loads as recommended in the seismic design code of the selected structures (Iranian code of practice for seismic resistant design of buildings, 2005). On the beams, the axial forces due to gravity loads were assumed to be equal to zero. The flexural inelastic behavior of the elements was considered in this study using lumped plasticity at both ends. A simplified bilinear moment-rotation curve was used for each plastic hinge

The commonly used confined concrete model proposed by Mander *et al.* (1988), was implemented while an elastic perfectly plastic model with parabolic strain hardening was considered for steel. The properties recommended in ASTM (ASTM A615M, 2009) were used for the steel reinforcement. The design properties of steel reinforcement and concrete were also used during the nonlinear analysis.

The ultimate condition (ultimate moment and ultimate curvature) was assumed to be the attainment of one of the following conditions; whichever happened earlier (Inel and Ozmen, 2006);

- 1) A 20% drop in the moment capacity of member,
- 2) When the tensile strain in the longitudinal steel reaches the ultimate tensile strain,
- 3) The attainment of the ultimate compression strain in concrete using Eqn. 3.1 proposed by Scott *et al.* (1982).

$$\varepsilon_{cu} = 0.004 + 0.9\rho_s \left( \frac{f_{yh}}{300} \right) \quad (3.1)$$

In the above equation,  $\varepsilon_{cu}$  is the ultimate compressive strain of concrete,  $\rho_s$  is the volumetric ratio of confining reinforcement and  $f_{yh}$  represents the yield strength of transverse steel.

Plastic rotation is defined as the difference between the ultimate and the yield curvature (curvature ductility) multiplied by the plastic hinge length. Many equations have been proposed by researchers for the plastic hinge length (Park and Paulay, 1975; Paulay and Priestley, 1992). In this study, the plastic hinge was calculated as:

$$L_p = H/2 \quad (3.2)$$

where  $L_p$  and  $H$  are the plastic hinge length and the height of section, respectively. This simple, yet adequately accurate relation for the plastic hinge length is also recommended by ATC-40 (ATC, 1996). It should be noted that according to Paulay and Priestley (1992), Eqn. 3.2 results in accurate values for conventional beam and column sections.

The axial-moment and flexural moment hinges were introduced at the end of columns and beams, respectively and the calculated nonlinear properties based on the section analysis were then imported to each hinge. For the columns, the yield moment changes according to the axial load. Thus, a yield moment-axial load interaction curve needs to be defined for each column.

### 3.2. Verification of the Modeling Assumptions

In order to validate the aforementioned assumptions for the quantification of the plastic hinge properties and the pushover results, two 2-D reinforced concrete frames which were studied by Filiatrault *et al.* (1998a, b) were selected. Each structure was assumed to be part of the lateral load resisting system of a building, with two stories (each 1.5 m high) and two bays (each 2.5 m wide). Herein, the pushover results of the ductile frame is selected in order to be compared with the defined hinge model characterized based on the assumptions of the previous section.

Similar to their analysis, the distribution of lateral loads in pushover analysis was identical to the one used for the design of the structures. Also, the full gravity load was applied to the structure. The plastic properties of defined hinges were calculated using member reinforcement and the assumed models for concrete and steel described in the previous section. For this quantification, the actual material properties obtained by Filiatrault *et al.* (1998a) from tensile test on reinforcing steel and compressive test on concrete cylinders were considered. The base shear versus roof lateral displacement (so-called pushover) curve obtained from SAP 2000 was compared with that of Filiatrault *et al.* (1998b) in Fig. 3.1. Considering the differences between the lumped and spread plasticity approach, the two load-displacement curves agree well, proving the accuracy of the above mentioned assumptions for the definition of plastic hinges. In particular, the failure points predicted by the two methods correspond to each other reasonably well.

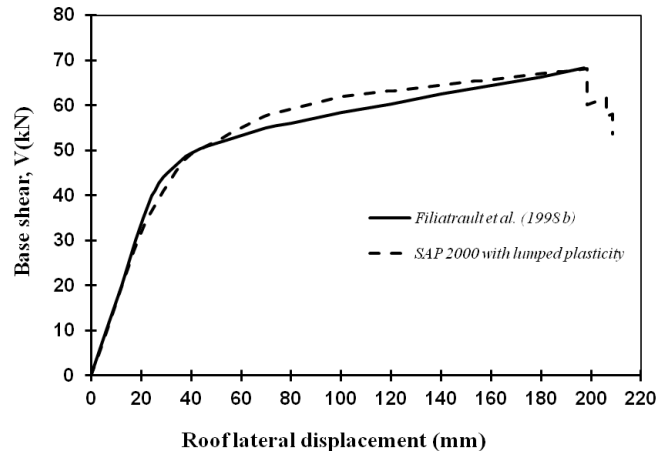


**Figure 3.1.** Comparison of pushover curves of ductile RC frame

### 3.3. Pushover Results of the Original Frames

Pushover analysis consists of an incrementally increasing lateral load applied to the structure up to the failure point in the presence of a constant gravity load. In this study, the total dead load plus 20% of the live load based on the Iranian seismic code (Iranian code of practice for seismic resistant design of buildings, 2005), is applied to the frame studied. For the seismic evaluation of a building, the lateral force profile applied to the building should represent, albeit approximately, the likely distribution of inertial forces induced during an earthquake. In the current paper, an inverted triangular distribution over the height is used as the lateral load pattern. This lateral load pattern provides better estimates of the capacity curve and seismic responses when compared with a uniform distribution. In addition, while inverted triangular distribution is more practical than multi-modal distribution, it would yield similar results (Mwafy and Elnashai, 2001). The effect of  $P-\Delta$  has also been considered in all nonlinear analyses.

Due to the flexural cracking of the RC members, the stiffness of the members is reduced during the seismic loads. The reduction in the flexural stiffness was calculated from the elastic part of the moment curvature curve of each section. On account of negligible effect of confinement on the yielding point, the stiffness ratio for both frames was calculated to be almost identical.

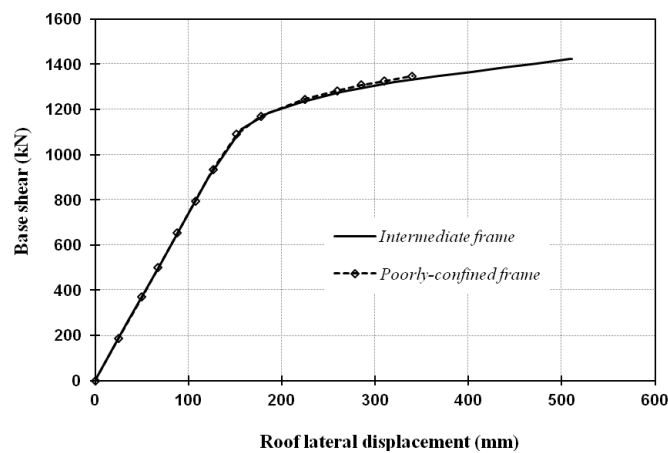


**Figure 3.2.** Lateral load-displacement curves of original frames

The lateral load-displacement curves obtained from the nonlinear pushover analyses of code-compliant and poorly-confined frames are compared in Fig. 3.2. While the lateral-load carrying capacities of two structures are identical, lower confinement resulted in a significant decrease (about 34%) in the displacement ductility in the poorly-confined frame. In addition, considering the pre-yielding and post-yielding stiffness, both frames behaved in a similar manner. The fact that the confinement of the members only increases the displacement capacity of the structures instead of stiffness, demonstrates the distinct advantage of retrofitting by FRP confinement. In the latter, the structure would attract higher seismic forces and hence the effectiveness of the retrofit is decreased.

#### 4. DESIGN OF COMPOSITE WRAPS

From the retrofitting point of view using composite material, it was decided to increase the displacement capacity of the structure and provide more energy dissipation under seismic loads. Following this objective, two retrofitting strategies were selected: (1) fully exploiting the rotational capacity of beams and columns through GFRP wrapping of columns in both code-compliant and poorly-confined frames and (2) increasing the ductility of beams in code-compliant structure in addition to column wrapping.

To provide confinement in the columns, glass fibres are more attractive than others. While they have the highest ultimate strain of any high modulus fibre, their low fatigue and creep rupture resistance are not a crucial factor in this type of application (De Luca *et al.*, 2011). A comparison between GFRP and CFRP material showed that the former provides more displacement ductility for the confined concrete with lower amount of composite material. In addition glass fibre materials are more cost effective than the carbon fibres. Thus the GFRP composite materials were considered for the confinement of columns in this study. The design properties of unidirectional glass fibre sheets as provided by the manufacturer are as follows: fibre thickness  $t_f = 0.589 \text{ mm}$  per layer, tensile modulus  $E_f = 72397 \text{ MPa}$ , ultimate tensile strain equal to 0.045, and ultimate tensile strength  $f_{tu} = 3241 \text{ MPa}$  (De Luca *et al.*, 2011). The stress-strain model proposed by Lam and Teng (2003a, b) was selected for FRP-confined concrete. A comprehensive investigation by the authors and other researchers (Rocca *et al.*, 2009) proved that this model is most suitable for predicting the maximum confined compressive strength and strain of circular and rectangular RC columns. Due to the effect of non-uniform stress distribution and curvature in the FRP jacket, the rupture strain of the FRP is lower than the ultimate tensile strain determined from direct coupon tests. Based on the evaluation of experimental data, Lam and Teng (2003a, b) suggested a value of 62.4% ultimate tensile strength for GFRP composites.

##### 4.1. Intermediate Frame

The first retrofitting configuration consisted of wrapping the column at the high seismic demand regions in order to provide more ductility capacity without changing the location of plastic hinges. During the nonlinear static analysis of the original frame, only plastic hinges in the columns of the bottom stories exhibited severe plastic behaviour. Thus the columns of the first four stories were wrapped with GFRP in the potential regions of plastic hinge formation. In addition, a sensitivity analysis confirmed that the GFRP confinement of the top columns would not affect the nonlinear response of the frame significantly. To quantify the amount of GFRP to be installed in the columns, the internal column at the first storey was selected since it carried the maximum axial force due to gravity loads and thus had the minimum rotational capacity. The composite thickness was calculated based on changing the column failure mode in the section analysis from concrete crushing to steel rupture. For the selected column, it could be achieved with four layers of GFRP sheets which increased the ultimate strain of column concrete to  $\varepsilon_{cu} = 0.0235$ . The effect of FRP confinement was taken into account by modifying the flexural inelastic behaviour of the elements at the member ends, where it was assumed that the nonlinear plastic hinges would be placed.

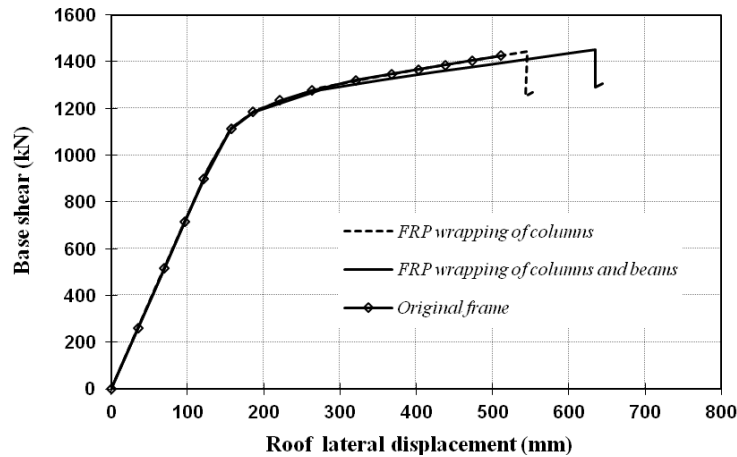


**Figure. 4.1.** Comparison of pushover curves of intermediate frame retrofitted using different FRP application

Fig. 4.1 compares the pushover curves of the retrofitted and the original frame. As expected, due to the adequate confinement provided through the transverse steel reinforcement, the additional confinement provided by composite material could not enhance the lateral displacement capacity significantly (roughly 7%). More exact evaluation of hinge damage state illustrated that a higher displacement capacity for the structure is achievable by increasing the rotational capacity of the plastic hinges at the lower beams. In order to pursue the second retrofitting technique; the plastic rotational capacity of hinges at the beams was increased by 24%. This value was selected from the average ductility enhancement in the code-compliant RC connections reported in the past studies (Mostofinejad and Talaeitaba, 2006; Talaeitaba, 2003). In the calculation of this mean value, those CFRP configurations that increase both the strength and stiffness have been neglected. The number and thickness of CFRP wrap to reach the targeted displacement ductility level could be calculated using the finite element analysis of the retrofitted joints. As observed in Fig. 4.1, more ductility capacity was provided for the intermediate frame with retrofitting both beams and columns of the first four stories. Retrofitting configurations that increase the load carrying capacity of this type of building might result in a higher seismic resistance. Discussion on this type of strengthening configuration is beyond the scope of this paper.

#### 4.2. Poorly-Confined Frame

Compared to the code-compliant building, the poorly-confined frame suffered from the inadequate transverse steel reinforcement resulting in low ductility capacity of the structure during the lateral loading. This represents the situation of many RC structures built based on the pre-seismic code provisions. In order to overcome this deficiency, using FRP wraps to provide additional confinement is an efficient rehabilitation method since it increases the ductility capacity without considerable strength increment. In this study, the efficiency of GFRP wraps to improve a displacement capacity of a poorly-confined frame to the levels seen in an intermediate frames is studied. For this purpose, the plastic rotation of columns is enhanced using FRP confinement of concrete. The columns of the first four stories were wrapped with four layers of GFRP, while three layers of GFRP wraps was applied on the columns of the other stories. Composite thickness in the bottom column was selected to be similar to the intermediate frame, while three layers of GFRP was calculated to be adequate to provide stress strain model for confined concrete similar to the bottom columns. In both column categories, the ultimate concrete strength and strain were  $f'_{cc} = 46\text{MPa}$  and  $\epsilon_{cu} = 0.0235$  respectively.

The lateral load-displacement curves obtained from the nonlinear static analyses of FRP-confined and original frames are compared in Fig. 4.2. The displacement capacity of frame was enhanced by approximately 38% using GFRP wrapping of columns. It is worth mentioning that FRP-confinement has no effect on the slope of the pushover curve before yielding. The nonlinear outcomes emphasized

the capability of column confinement in improving the seismic performance of deficient RC building with inadequate transverse reinforcement.

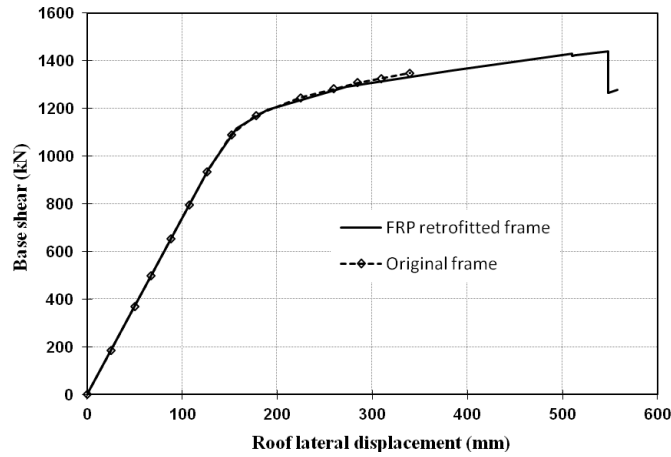


Figure. 4.2. Comparison of pushover curves for poorly-confined frame

## 5. SEISMIC ASSESSMENT OF THE RETROFITTED STRUCTURE

The capacity diagrams, obtained using the pushover analysis of the original and retrofitted frames, could be compared with the demand spectrum to assess the seismic performance of structures at different levels of ground motion. In this study, amongst different methods developed, the N2 method (Fajfar, 2000) was employed for the seismic analysis of the poorly-confined frame. The method is formulated in acceleration-displacement (AD) format with a visual representation of the procedure. Seismic demand was defined with the elastic response spectrum (soil type III, 5% damping) suggested for the design of structures in the Iranian seismic code (Iranian code of practice for seismic resistant design of buildings, 2005). In the capacity spectrum approach, the elastic acceleration ( $S_{ae}$ ) and displacement spectrum ( $S_{de}$ ) are plotted in AD format in order to calculate the seismic demand of the equivalent SDOF system. Neglecting the performance level restrictions, the maximum sustainable ground motion for the equivalent SDOF systems of the original and retrofitted frame was calculated using the N2 method to be 0.32g and 0.52g, respectively. These peak ground accelerations were calculated using a feedback procedure to achieve the same elastic displacement demand and elastic displacement capacity for equivalent SDOF. The capacity curve obtained from the pushover analysis was transformed from the MDOF system to an equivalent SDOF. The transformation factor is given by:

$$\Gamma = \frac{\sum m_i \phi_i}{\sum m_i \phi_i^2} \quad (5.1)$$

where  $m_i$  and  $\phi_i$  are the mass and normalized displacement of the  $i$ th story.

Assuming an equal mass for all stories, the displacement distribution pattern is similar to the lateral load distribution and the transformation factor was calculated to be 1.41. The seismic demand for the equivalent SDOF system could be determined by plotting both demand spectra and capacity diagram in the same graph. The intersection of radial line corresponding to the elastic period of the idealized bilinear system,  $T^*$ , with the elastic demand spectrum determines the acceleration demand and corresponding displacement demand required for the elastic behaviour. The amount of ductility factor,  $\mu$  depends on whether,  $T^*$  is larger or smaller than the characteristic period of ground motion,  $T_c$ . The inelastic demand of SDOF system in terms of acceleration and displacement is defined by the intersection of the idealized capacity curve and the inelastic demand spectrum corresponding to  $\mu$ . The displacement demand of the MDOF system is obtained by multiplying the SDOF demand by the

transformation factor. Fig. 5.1 provides a graphical demonstration of the N2 method for the poorly-confined frame. The requested ductility for the PGA of 0.52g and 0.32g was equal to 3 and 1.97, respectively. As observed from the idealized bilinear capacity curves, the available structural ductility of the original frame increased by 52% after FRP application. This resulted in an increase in the seismic load capacity to the PGA of 0.52g instead of 0.32g.

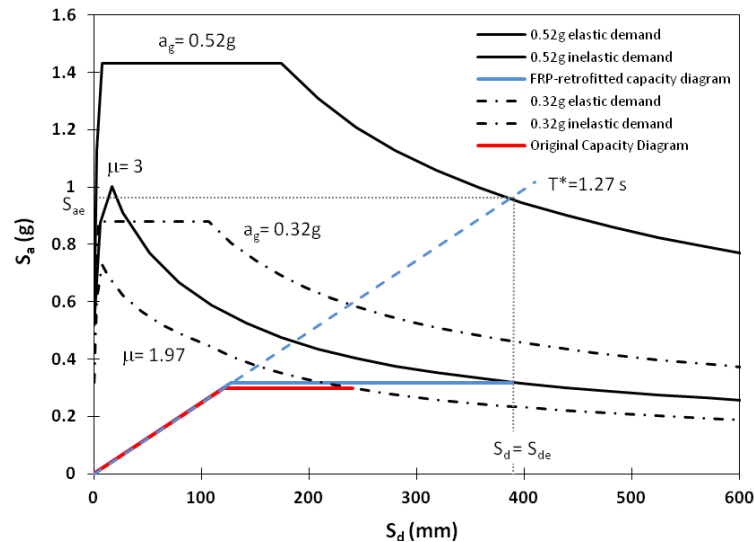


**Figure. 5.1.** Demand spectra vs. capacity diagrams of poorly-confined frame using the N2 method

## 6. CONCLUSIONS

Retrofitting strategy in this study was focused on increasing the ductility instead of strengthening using FRP wrapping. Plastic behaviour of the elements was characterized using two nonlinear hinges at the end sections of the members based on the lumped plasticity concept. After verification of the adopted assumptions for nonlinear characterization of members, the results of pushover analysis were implemented in seismic assessment of frames.

Nonlinear analyses' results outlined the inefficiency of column wrapping in improving the ductility of code-compliant structures. This is particularly due to the adequate lateral confinement provided by transverse steel reinforcements. For the intermediate frame, increasing the beam ductility appears to be more effective. However, FRP wraps could enable the poorly confined structure to resist much higher ground motion (PGA= 0.52g) through increasing the ductility and energy dissipation capacity. More studies need to be conducted on the FRP-retrofitting of RC frames detailed based on the older versions of building design codes in order to improve the understanding of their behaviour and, as such, to provide a more economical retrofitting scheme for this type of buildings against the more stringent demands set by the recent codes.

## ACKNOWLEDGMENT

The authors gratefully thank Imbsen & Associate, *Inc.* for providing a free license for the XTRACT software (Imbseon and Associates *Inc.*, 2011)

## REFERENCES

- ACI Committee 318 (2002). Building code requirements for structural concrete (ACI 318-02) and commentary (ACI 318R-02). Farmington Hills, Mich.: American Concrete Institute.
- American Society of Civil Engineering (ASCE) (2000). Prestandard and commentary for the seismic rehabilitation of buildings (FEMA-356). Washington, DC: Federal Emergency Management Agency.

- ASTM A615M (2009). Standard specification for deformed and plain carbon-steel bars for concrete reinforcement. Philadelphia, Pa. : American Society for Testing and Materials.
- ATC (1996). Seismic evaluation and retrofit of concrete buildings(ATC-40). California: Applied Technology Council.
- Balsamo, A., Colombo, A., Manfredi, G., Negro, P. and Prota, A. (2005). Seismic behavior of a full-scale RC frame repaired using CFRP laminates. *Engineering Structures*, 27:5, 769-780.
- Computers and Structures Inc (2009). Static and dynamic finite element analysis of structures. *SAP 2000*. 14.1.0 ed. Berkeley (CA); .
- De Luca, A., Nardone, F., Matta, F., Nanni, A., Lignola, G. P. and Prota, A. (2011). Structural evaluation of full-scale FRP-confined reinforced concrete columns. *Journal of Composites for Construction*, 15:Compendex, 112-123.
- Di Ludovico, M., Prota, A., Manfredi, G. and Cosenza, E. (2008). Seismic strengthening of an under-designed RC structure with FRP. *Earthquake Engineering & Structural Dynamics*, 37:1, 141-162.
- Fajfar, P. (2000). A nonlinear analysis method for performance-based seismic design. *Earthquake Spectra*, 16:Compendex, 573-592.
- Filiatrault, A., Lachapelle, E. and Lamontagne, P. (1998a). Seismic performance of ductile and nominally ductile reinforced concrete moment resisting frames. I. Experimental study. *Canadian Journal of Civil Engineering*, 25, 331-341.
- Filiatrault, A., Lachapelle, E. and Lamontagne, P. (1998b). Seismic performance of ductile and nominally ductile reinforced concrete moment resisting frames. II. Analytical study. *Canadian Journal of Civil Engineering*, 25, 342-352.
- Imbseon and Associates Inc (2011). Cross section analysis program for structural engineers. *XTRACT*. 3.0.8 ed. California; .
- Inel, M. and Ozmen, H. B. (2006). Effects of plastic hinge properties in nonlinear analysis of reinforced concrete buildings. *Engineering Structures*, 28:11, 1494-1502.
- Lam, L. and Teng, J. G. (2003a). Design-oriented stress-strain model for FRP-confined concrete. *Construction and Building Materials*, 17:6-7, 471-489.
- Lam, L. and Teng, J. G. (2003b). Design-oriented stress-strain model for FRP-confined concrete in rectangular columns. *Journal of Reinforced Plastics and Composites*, 22:Compendex, 1149-1186.
- Mander, J. B., Priestley, M. J. N. and Park, R. (1988). Theoretical stress-strain model for confined concrete. *Journal of Structural Engineering*, 114:Compendex, 1804-1826.
- Mostofinejad, D. and Talaeitaba, S. B. (2006). Finite element modeling of RC connections strengthened with FRP laminates. *Iranian Journal of Science and Technology, Transaction B: Engineering*, 30:GEOBASE, 21-30.
- Mwafy, A. M. and Elnashai, A. S. (2001). Static pushover versus dynamic collapse analysis of RC buildings. *Engineering Structures*, 23:5, 407-424.
- Niroomandi, A., Maheri, A., Maheri, M. R. and Mahini, S. S. (2010). Seismic performance of ordinary RC frames retrofitted at joints by FRP sheets. *Engineering Structures*, 32:8, 2326-2336.
- Park, R. and Paulay, T. (1975). Reinforced concrete structures, New York, Wiley.
- Paulay, T. and Priestley, M. J. N. (1992). Seismic design of reinforced concrete and masonry buildings, New York, Wiley.
- Permanent Committee for Revising the Iranian Code for Seismic Resistant Design of Buildings (2005). Iranian code of practice for seismic resistant design of buildings (Standard No. 2800-05). 3rd ed. Tehran (Iran): Building and Housing Research Center (BHRC).
- Rocca, S., Galati, N. and Nanni, A. (2009). Interaction diagram methodology for design of FRP-confined reinforced concrete columns. *Construction and Building Materials*, 23:4, 1508-1520.
- Scott, B. D., Park, R. and Priestley, M. J. N. (1982). Stress-strain behavior of concrete confined by overlapping hoops at low and high strain rates. *Journal of the American Concrete Institute*, 79:Compendex, 13-27.
- Talaeitaba, S. B. (2003). Ductility enhancement of RC joints with FRP laminates. M.Sc Thesis (In Farsi), Isfahan University of Technology (IUT), Isfahan, Iran.